Potential Predictability of Seasonal Means Based on Monthly Time Series of Meteorological Variables

XIAOGU ZHENG

National Institute of Water and Atmospheric Research, Wellington, New Zealand

HISASHI NAKAMURA

IGCR, Frontier Research System for Global Change, and Department of Earth and Planetary Physics, University of Tokyo, Tokyo, Japan

JAMES A. RENWICK

National Institute of Water and Atmospheric Research, Wellington, New Zealand

(Manuscript received 3 May 1999, in final form 12 October 1999)

ABSTRACT

Based only on monthly mean data, an analysis of variance method is proposed for decomposing the interannual atmospheric variability in seasonal-mean time series into components related to ''weather noise'' and to slowly varying boundary forcing and low-frequency internal dynamics. The ''potential predictability'' is then defined as the fraction of the total interannual variance accounted for by the latter two components. A study using synthetic data showed that the method proposed here is comparable in performance to conventional methods requiring daily data.

The technique was applied to gridded global data of monthly surface temperature, 500-hPa height, and 300-hPa wind in order to examine the geographical and seasonal dependencies of their potential predictability. For all the variables, the highest potential predictability tends to be found in the Tropics, where seasonal anomalies in the atmosphere are strongly coupled with the underlying sea surface temperature anomalies and the weather noise component is relatively weak. In contrast, the predictability is generally low over the extratropics. Surface temperature, however, exhibits relatively high predictability over the subtropical and midlatitude oceans, particularly over the midlatitude North Pacific in winter, where the El Niño–Southern Oscillation events exert strong influences through atmospheric teleconnection. These results appear physically reasonable and consistent with our current understanding based on previous observational and model-based analyses.

1. Introduction

Monthly and seasonal mean time series of meteorological variables are widely used for analyzing interannual climate variability and predictability, using either observed time series or the output of general circulation models (GCMs). Studies of predictability and potential predictability are usually based upon decomposition of temporal variability into a part called the ''weather noise'' variability that is fundamentally unpredictable on seasonal timescales and another part assumed to be at least potentially predictable (Madden 1976). The potential predictability is often measured as the fraction of the total variability accounted for by the latter part. Such measures are clearly sensitive to how the separation of variance is performed. In many cases, temporal filtering techniques are employed on the assumption that weather noise operates mainly on timescales much shorter than that of the potentially predictable variability (e.g., Basher and Thompson 1996). However, weather events include not only high-frequency, day-to-day fluctuations but also low-frequency intraseasonal fluctuations that give rise to chaotic, unpredictable fluctuations in seasonal-mean time series. Therefore, it is not possible to completely isolate the potentially predictable variability through temporal filtering.

A framework useful for analysis of climate variability and predictability is to consider seasonal mean time series to be made up of the following three components: a forced component, an internal source component, and a residual weather noise component (e.g., Lorenz 1970; Leith 1973; Zwiers 1996; Zheng and Frederiksen 1999). The forced component represents the atmospheric re-

Corresponding author address: Xiaogu Zheng, National Institute of Water and Atmospheric Research, P.O. Box 14901, Kilbirnie, Wellington, New Zealand.
E-mail: x.zheng@niwa.cri.nz

sponse to gradual changes in the atmospheric composition, particularly in greenhouse gas concentration (e.g., Manabe et al. 1991, 1992) and to slowly varying boundary conditions such as sea surface temperature (SST) anomalies (Bjerknes 1969; Rowntree 1972; Horel and Wallace 1981; Lau and Nath 1994; Shukla 1998) and anomalous sea-ice cover (Honda et al. 1999). The internal source component represents low-frequency atmospheric variability induced by atmospheric internal dynamics. The equatorial stratospheric quasi-biennial oscillation is a particularly striking example (Holton 1992). Interannual variability in the extratropics associated with stationary circulation anomalies, such as the North Atlantic oscillation (NAO; van Loon and Rodgers 1978; Wallace and Gutzler 1981; Kushnir and Wallace 1989) and the Pacific/North American (PNA) pattern (Wallace and Gutzler 1981; Kushnir and Wallace 1989), may be influenced by internal dynamics including persistent feedback forcing from synoptic-scale eddies traveling along anomalous storm tracks (Lau 1988; Lau and Nath 1991; Hurrel 1995). Extratropical remote response to the El Niño–Southern Oscillation (ENSO; e.g., Rasmusson and Carpenter 1982; Cane 1986; Kleeman and Moore 1997) may also be modulated by such a feedback from transient eddies (Hoerling and Ting 1994).

The forced and internal source components of the atmospheric variability are, by nature, (nearly) constant within a season, whereas the weather noise component includes fluctuations over a wide range of frequencies. The weather noise component should average to zero if sampled over a very large number of realizations, but not necessarily so if averaged over a single season. Since the power spectrum of large-scale atmospheric motions is fundamentally red, a nonzero seasonal mean of the weather noise component is largely contributed to by intraseasonal weather events with monthly or longer timescales, including persistent blocking events in the extratropics and the Madden–Julian oscillation (MJO) in the Tropics (Madden and Julian 1971, 1972). Transient eddies along storm tracks, whose characteristic timescales are less than 10 days, tend to exert only a small direct influence upon the weather noise component in monthly or seasonal means (Blackmon et al. 1984), although, as mentioned earlier, their indirect influence may be significant through their feedback on disturbances with lower frequency. An important difference between the forced and internal source components is that the latter are very sensitive to initial conditions while the former are not.

The above variance decomposition may apply in most areas of climate variability research. An important application may be found in the assessment of potential long-range predictability of the atmospheric circulation, that is, the predictability of seasonal means a season or more in advance (Madden 1976, 1981). As mentioned above, the potential predictability may be measured as the fraction of the total variability in seasonal means accounted for by the potentially predictable forced and internal source components. Dominance of the seasonally unpredictable variability associated with the weather noise component therefore lowers the potential predictability.

Another useful application may be found in validation of the skill of atmospheric GCMs, in particular in terms of the model's ability to reproduce the forced component. Model skill is often evaluated as the correlation between raw seasonal anomalies in the observation and a model simulation. Yet, their correlation based only on the forced component, if successfully estimated, should become a more precise measure of the model's performance. Furthermore, ensemble GCM experiments subject to an identical prescribed forcing with various initial conditions should, in theory, enable separation of the variability due to the forced component from that due to the internal source component, which may lead to deeper understanding of the influence of (nonlinear) internal dynamics on climate variability (Zwiers 1996; Zheng and Frederiksen 1999).

Correctly estimating the variability due to the weather noise component is crucial to the two applications mentioned above (Zheng and Frederiksen 1999). Typically, the estimation requires a daily time series and an assumption of its normality (Jones 1975; Madden 1976; Trenberth 1984; Zwiers 1987; Zheng 1996). These requirements, however, are subject to two main limitations. First, daily time series of many meteorological variables cannot be regarded as normally distributed. For example, the frequency distribution of daily wind speed or rainfall is highly skewed. Second, availability of daily time series is limited in comparison with that of monthly time series. For example, surface observations were recorded on a daily basis rarely during the early instrumental period, and many modeling groups record monthly statistics only. Therefore, it would be very useful to develop a method for estimating the variability due to the weather noise component based only on monthly mean time series.

In this paper, analysis of variance approaches are proposed for estimating the potentially predictable and weather noise variability separately, only from normally distributed monthly means. A method is also described for subsequent testing of potential predictability based on Zheng (1996) and Zwiers (1996). Monthly means were used by Zwiers (1996) for estimating interannual variability due to the weather noise component. Daily data were still required, however, to evaluate the correlation of the component between two adjacent months. The proposed method is then applied to assessing the potential predictability of global surface temperatures and the mid- and upper-tropospheric circulation. An analysis of synthetic red noise data demonstrates that the proposed estimation approach is comparable to the popular approach proposed by Zwiers (1987), which requires daily data.

The present paper begins with a description of the proposed variance estimation method and evaluation of

the potential predictability. Section 3 is devoted to applications to monthly fields of observed meteorological data. A summary and conclusions are presented in section 4. Mathematical details and a comparative analysis of synthetic data and meteorological data are discussed in the appendixes.

2. Methodology

In the discussion to follow, it is assumed that the mean annual cycle has been removed by a harmonic equivalent analysis (e.g., Epstein 1991). Any uncertainties introduced by the estimation of the mean annual cycle are ignored. In this study, a season is assumed to be 3 months long, but the method described may easily be applied to ''seasons'' of any length.

a. Statistical model

The basic statistical model for monthly means of a variable (x) for a particular season obtained over a number of years (Y) may be expressed in the following linear regression form:

$$x_{ym} = \mu_y + \varepsilon_{ym}, \tag{1}$$

where y ($=1, \ldots, Y$) denotes the year, m ($=1$, 2, or 3) a month within a given 3-month season, μ_y a seasonal anomaly in year y due to boundary forcings, radiative forcings and slowly varying internal dynamics, and ε_{ym} a residual monthly departure of x_{ym} from the seasonal value μ_y. The residual weather noise component, which consists of $\{\varepsilon_{y1}, \varepsilon_{y2}, \varepsilon_{y3}\}$, is assumed to comprise a three-dimensional stationary stochastic process in time with zero means and to be statistically independent and identically distributed with respect to year y. The model (1) is similar to the one described in the introduction, but in (1) the forced and internal source components are combined into μ_y. This combination is necessary because one cannot isolate the internal source component from the boundary-forced component in the observed time series (a single realization of the climate system). Still, ensemble GCM simulations should allow such a separation to be achieved, by utilizing the strong sensitivity of the internal source component to initial conditions [see Zwiers (1996) and Zheng and Frederiksen (1999) for more details].

Throughout this paper, we represent an average taken over an independent variable (i.e., m or y) by replacing that variable indicated as subscript with ''o.'' For example, x_{yo} indicates the 3-month average of x_{ym} in year y and x_{oo}, the average of x_{ym}, taken over all 3 months and all Y years. With this notation, a seasonal mean can be expressed as

$$x_{yo} = \mu_y + \varepsilon_{yo}. \tag{2}$$

As in Zheng and Frederiksen (1999), a symbol V denotes the variance of a single variable or the covariance between two variables and another symbol C the correlation coefficient between two variables, all of which are evaluated over all Y years. Estimated quantities are indicated with a circumflex ''^.'' For example, $\hat{C}(\varepsilon_{y1}, \varepsilon_{y2})$ represents the estimated correlation coefficient between ε_{y1} and ε_{y2}.

The following assumptions about monthly values of the weather noise component in (1) are necessary for estimating its variance $V(\varepsilon_{yo})$. Since its daily time series within a season is, in general, assumed to be stationary, so are the monthly statistics. Specifically, its interannual variance is assumed to be independent of months, that is,

$$V(\varepsilon_{y1}) = V(\varepsilon_{y2}) = V(\varepsilon_{y3}), \tag{3}$$

and so is its intermonthly covariance, that is,

$$V(\varepsilon_{y1}, \varepsilon_{y2}) = V(\varepsilon_{y2}, \varepsilon_{y3}). \tag{4}$$

Strictly speaking, these assumptions may not apply well in transition seasons, but they are probably reasonable for winter or summer seasons as in this study. Recognizing that day-to-day weather events are unpredictable beyond a week or two, we further assume that monthly means of the weather noise component are uncorrelated if they are a month or more apart. For 3-month seasons,

$$V(\varepsilon_{y1}, \varepsilon_{y3}) = 0. \tag{5}$$

Furthermore, $\varepsilon_{y1} - \varepsilon_{y2}$ and $\varepsilon_{y2} - \varepsilon_{y3}$ are assumed to be normally distributed. This assumption is weaker than the assumption that all ε_{ym} are normally distributed (Rao 1973). Here, since month-to-month fluctuations arise entirely from the weather noise component (i.e., $\varepsilon_{y1} - \varepsilon_{y2} = x_{y1} - x_{y2}$), we can check the normality assumption directly from observed monthly data. We confirmed that the normality condition is approximately satisfied for monthly means of such variables as temperature, pressure, and wind speed, but not for monthly rainfall.

b. Variance estimates

We have derived specific expressions of the estimated statistics in (1) and (2), which are listed in Table 1. Some details in the derivations are presented in appendix A. The intermonthly correlation of the weather noise component $\hat{C}(\varepsilon_{y1}, \varepsilon_{y2})$, which is the key statistic in calculating others, has been derived through a maximum likelihood estimation similar to that documented in Zheng (1996) and Zwiers (1996), with a constraint that the correlation lies between 0 and 0.1. For such a continuous meteorological variable as pressure and temperature (but not precipitation), its daily time series can roughly be regarded as AR(1), a first-order autoregressive process (Trenberth 1984; Zwiers and von Storch 1995; Zwiers 1996), characterized by the first-order autocorrelation coefficient α, which is generally between 0 and 0.9. For a daily AR(1) time series, the correlation coefficient of its mean between two adjacent months is approximately given by

TABLE 1. Formulas for parameter estimates.

$\hat{V}(x_{yo})$	$\frac{1}{Y-1}\sum_{y=1}^{Y}(x_{yo}-x_{oo})^2$
$\hat{C}(\varepsilon_{y1}, \varepsilon_{y2}) = \hat{C}(\varepsilon_{y2}, \varepsilon_{y3})$	$\min\{0.1, \max[1.5 - v_1/v_2, 0]\}$
$\hat{C}(\varepsilon_{y1}, \varepsilon_{y3})$	0
$\hat{V}(\varepsilon_{ym})$, $m = 1, 2, 3$	$\frac{-2v_2\hat{C}(\varepsilon_{y1}, \varepsilon_{y2}) + 2v_1}{3 - 4\hat{C}(\varepsilon_{y1}, \varepsilon_{y2})}$
$\hat{V}(\varepsilon_{yo})$	$\frac{\hat{V}(\varepsilon_{y1})[3 + 4\hat{C}(\varepsilon_{y1}, \varepsilon_{y2})]}{9}$
$\hat{V}(\mu_y)$	$\hat{V}(x_{yo}) - \hat{V}(\varepsilon_{yo})$
v_1	$\frac{1}{2Y}\sum_{y=1}^{y}\left[\sum_{m=1}^{3}x_{ym}^2 - \sum_{m_1\neq m_2}x_{ym_1}x_{ym_2}\right]$
v_2	$\frac{1}{2Y}\sum_{y=1}^{y}(x_{y1} - x_{y3})^2$

$$C(\varepsilon_{y1}, \varepsilon_{y2}) \approx \frac{\alpha}{900(1-\alpha)^2} \tag{6}$$

(Zwiers 1996). Substituting 0 and 0.9 to α in (6) yields 0 and 0.1 as the lower and upper bounds for $\hat{C}(\varepsilon_{y1}, \varepsilon_{y2})$, respectively.

c. A test for potential predictability

In the statistical model (2), a seasonal mean x_{yo} conceptually consists of μ_y and ε_{yo}. As mentioned earlier, the potential predictability of the former may be measured as the ratio $V(\mu_y)/V(x_{yo})$. For assessing the level of its statistical significance, however, it is convenient to consider $V(x_{yo})/V(\varepsilon_{yo})$ rather than $V(\mu_y)/V(x_{yo})$. A high significance level implies high potential predictability of observed seasonal means. Otherwise, they are dominated by the weather noise component and hence considered unpredictable.

With the estimated variance of ε_{yo} as given in Table 1, the statistical significance of the potential predictability of seasonal means can be assessed as follows. Since $C(\varepsilon_{y1}, \varepsilon_{y2})$ is constrained between 0 and 0.1 and $C(\varepsilon_{y1}, \varepsilon_{y3})$ is zero, $\hat{V}(\varepsilon_{yo})$ is approximately distributed as $\chi^2(2Y)V(\varepsilon_{yo})/(2Y)$, where $\chi^2(2Y)$ is the chi-square random variable with $2Y$ degrees of freedom (DOF; appendix A). Under the null hypothesis of no interannual variability arising from boundary forcings and slowly varying internal dynamics, that is, μ_y is identical for every $y = 1, 2, \ldots, Y$, the statistic

$$\frac{1}{Y-1}\sum_{y=1}^{Y}(x_{yo} - x_{oo})^2 = \frac{1}{Y-1}\sum_{y=1}^{Y}(\varepsilon_{yo} - \varepsilon_{oo})^2 \tag{7}$$

is distributed as $\chi^2(Y-1)V(\varepsilon_{yo})/(Y-1)$. The statistic in (7) becomes asymptotically independent of $\hat{V}(\varepsilon_{yo})$ as Y increases. Then the probability density distribution of the statistic

$$R = \frac{1}{Y-1}\sum_{y=1}^{Y}(x_{yo} - x_{oo})^2/\hat{V}(\varepsilon_{yo}) \tag{8}$$

is approximated by $F(Y-1, 2Y)$, the F distribution with DOFs of $Y-1$ and $2Y$, which has the mean $Y/(Y-1) \approx 1$. If R differs significantly from 1 at the α percent level, we claim the potential predictability is significant at that level.

3. Results

a. Surface air temperature

The temperature data used here are monthly mean surface temperature records archived on a regular 5° latitude by 5° longitude grid by the Climate Research Unit (CRU), the University of East Anglia (Jones 1996). They cover 106 yr since 1890, based on daily station data of surface air temperature (SAT) over land and in situ ship measurements of SST over the ocean. The record length is unevenly distributed in space, from 106 yr over Europe to less than 30 yr over the polar regions. Any grid point at which the observed record is available only for less than 30 yr has been excluded from our analysis. Most of these points are located poleward of 70°N or 80°S.

Before calculating subsequent variance estimates, a linear trend has been removed at each grid point since detection or analysis of trends is not a focus of this paper. A trend estimate depends rather strongly on the record length available, implying that the trend removal may leave significant uncertainties in the estimated forced/internal source variability in regions where the available record is relatively short. However, the trend removal should have no significant effect on the estimation of weather noise variability.

The estimated standard deviations of ε_{yo} and μ_y and the potential predictability of the latter are mapped in Fig. 1 for boreal summer (JJA) and winter (DJF) seasons. For presentation, most of the high-latitude data gaps have been filled in using a local regression interpolation. Variability in surface temperature due to the weather noise component tends to be stronger over land than over the ocean, which reflects the smaller heat capacity of the land surface. Over the mid- and high-latitude continents in the Northern Hemisphere, as is well known, the standard deviation is nearly twice as large in winter as in summer. This wintertime variability is attributed to strong intraseasonal transient activities such as blocking events that not only enhance warm and cold temperature advection but also act to form and destroy near-surface stratifications over cold continental surfaces. The opposite seasonal tendency is found in the

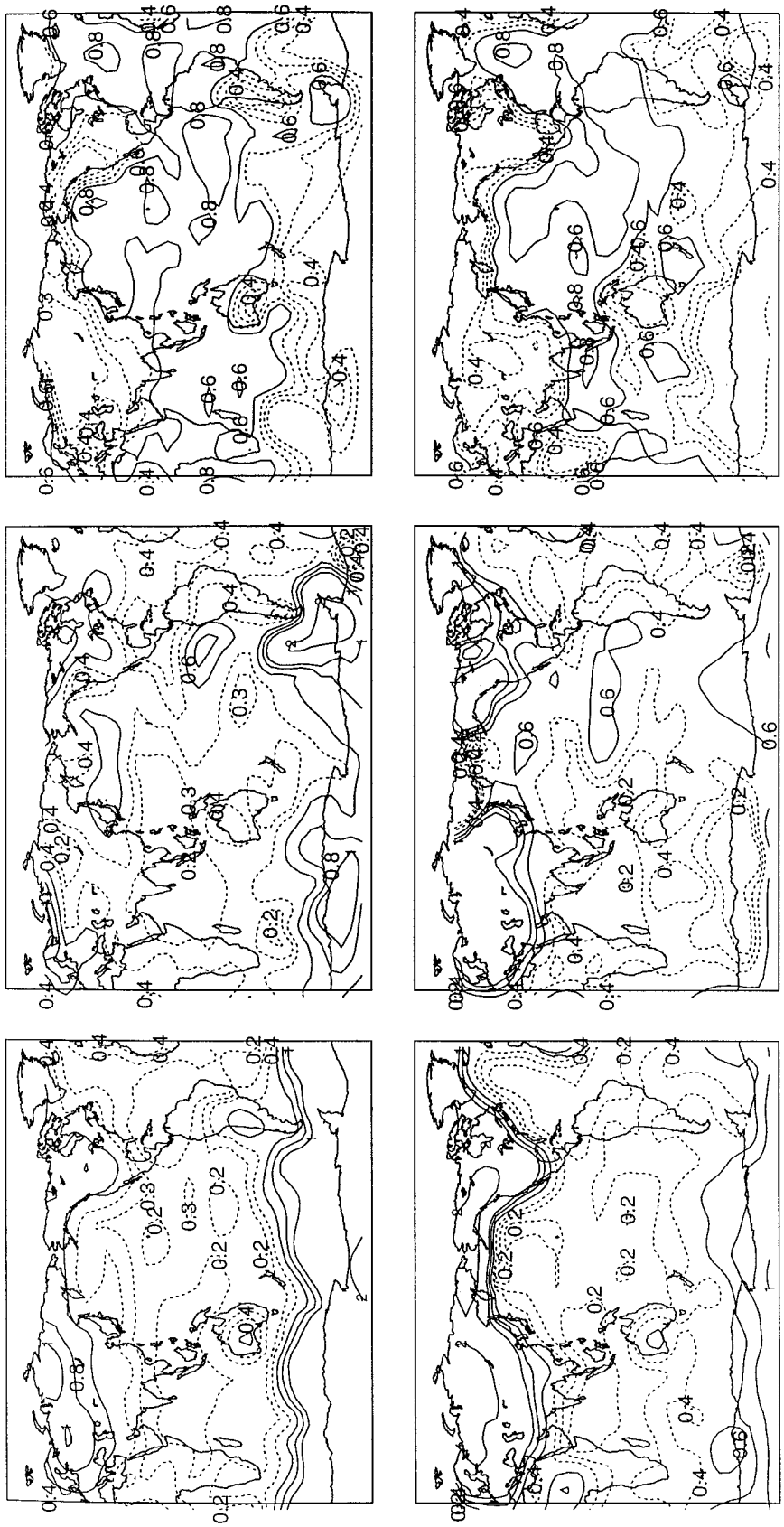

FIG. 1. Decomposition of the interannual variability in surface temperature based on the CRU SAT/SST data for (top) boreal summer and (bottom) winter into the variability associated with the weather noise component as measured by $\sqrt{V(\varepsilon_{yo})}$ (left) and that with the forced and internal source components combined as measured by $\sqrt{V(\mu_y)}$ (middle). Solid contours for 0.6°, 0.8°, and 1.0° and dashed contours for 0.2°, 0.3°, and 0.4°. A linear trend has been removed at each location. Also shown is the potential predictability of surface temperature as measured by $\hat{V}(\mu_y)/\hat{V}(\mu_y + \varepsilon_{yo})$ (right). Solid contours for every 0.1 from 0.5 to 0.9 and dashed contours for 0.3 and 0.4. The confidence levels of the estimated predictability are approximately 90%, 97%, and 99.5% for the variance ratio $\hat{V}(\mu_y)/\hat{V}(\mu_y + \varepsilon_{yo}) = 0.3$, 0.4, and 0.5, respectively.

weak weather noise component of extratropical SST.[1] In winter, $V(\varepsilon_{yo})$ is suppressed due to the large heat capacity of the oceanic mixed layer that is developed through the thermal and mechanical forcing by vigorous atmospheric intraseasonal disturbances, whereas the mixed layer shallows in summer acting to enhance the variability (Alexander and Deser 1995).

The overwhelming weather noise variability in SAT over the extratropical continents renders the potential predictability of SAT substantially lower than that of SST, despite the forced component being weaker in SST than in SAT, particularly over the wintertime continents. The potential predictability is particularly high in the equatorial Pacific, where the ENSO signal dominates over the weather noise component. The predictability is also particularly high in the wintertime extratropical North Pacific, where the prevailing upper-level westerlies allow effective teleconnection from the Tropics that enhances the remote influence of ENSO (Horel and Wallace 1981; Lau and Nath 1994). The relatively low predictability over the Southern Hemisphere maritime regions is primarily due to the relatively large $V(\varepsilon_{yo})$, which possibly reflects uncertainties in the data due to insufficient observations.

b. Tropospheric circulation

We use monthly mean global fields of 500-hPa height (Z500) and 300-hPa wind components (U300 and V300) over the period 1958–96, based on the National Centers for Environmental Prediction–National Center for Atmospheric Research (NCEP–NCAR) reanalyses (Kalnay et al. 1996). The data were subsampled on a regular $5^\circ \times 5^\circ$ latitude–longitude grid. Artificial climate ''jumps'' are minimized in the reanalyses by the use of a fixed assimilation/modeling system, but jumps and/or trends due to changes in observation systems may still be present (e.g., Kidson 1999). As above, a linear trend component fitted to the data time series has been removed at each grid point.

The estimated standard deviations of ε_{yo} and μ_y, and the potential predictability for Z500, U300, and V300 are mapped in Figs. 2–4, respectively. Intraseasonal variability in mid- and upper-tropospheric circulation is, in general, influenced by thermal conditions at the underlying surface to a much lesser degree than that in SAT or SST. Its distribution also reflects the land–sea thermal contrasts to a much lesser degree and hence should be more uniform in the zonal direction than that in SAT or SST. Still, weak zonal asymmetries are evident in weather noise variability in all fields, as described by Blackmon et al. (1984) for the Northern Hemisphere (NH) and by Trenberth (1981, 1982) for the Southern Hemisphere (SH). The variability itself and its zonal asymmetries both tend to be stronger in the winter hemisphere than in the summer hemisphere (Blackmon 1976; Trenberth 1982). The maximum over the far southeast Pacific is in the predominant blocking region identified by Sinclair (1996) and Renwick (1998). The weather noise variability is quite weak in the Tropics throughout the year.

Over NH, the wintertime weather noise variability in Z500 is strongest within the main jet exit regions, in good agreement with Blackmon (1976) and Blackmon et al. (1984). The strongest variability in summer appears in the polar region. In contrast to the weather noise variability, the ''forced'' variability in Z500 is distributed more or less uniformly. In the extratropics, the variability tends to be larger during winter in both hemispheres, but the seasonality is much more pronounced in NH. The prominent maxima over the far North Atlantic and central North Pacific correspond to the NAO and PNA, respectively, two of the most dominant anomaly patterns in the interannual timescales (Kushnir and Wallace 1989). The potential predictability of Z500 exhibits a pronounced tropical–extratropical contrast with much higher predictability in the Tropics than in higher latitudes, which reflects the suppression and predominance of the weather noise component in those two regions, respectively. Modest wintertime maxima in the predictability over the North Atlantic and North Pacific correspond to the NAO and PNA-like signals, respectively. The latter may manifest remote influence of ENSO via atmospheric teleconnection (Horel and Wallace 1981). The high predictability around Antarctica may be artificial due to the lack of observations, but it may in part reflect the interannual signal of the so-called Antarctic circumpolar wave (White and Peterson 1996).

Geographical and seasonal characteristics similar to those for Z500 apply to the estimated variance of the weather noise component in U300 and V300. Weaker tropical–extratropical contrasts in the wind variability than in the height variability are attributed to the breakdown of geostrophy in the Tropics. In the deep Tropics the influence of MJO leads to the dominance of U300 over V300 in the weather noise component (Madden and Julian 1971, 1972). Since extratropical fluctuations in U300 are associated primarily with quasi-stationary height anomalies with meridional dipole-like structure in jet exit regions (Blackmon et al. 1984; Kushnir and Wallace 1989), pronounced U300 variability due to the weather noise component is found in the central North Pacific and Atlantic. In contrast, extratropical V300 variability is associated primarily with wavelike anomalies. Distribution of the weather noise variability in V300 seems to reflect the seasonal characteristics of the mean flow in the extratropical SH with a single, zonally ex-

[1] Several studies have shown that the total interannual variability $V(x_{yo})$ in extratropical SST tends to be larger in summer than in winter (Cayan 1980; Iwasaka et al. 1987; Nakamura and Yamagata 1999), probably for the same reason as mentioned in the text. Our analysis indicates that the same tendency applies separately to each of the forced and weather noise components.

FIG. 2. As in Fig. 1, but for Z500 based on the NCEP–NCAR reanalyses. Here $\sqrt{\tilde{V}(\varepsilon_{yo})}$ (left) and $\sqrt{\tilde{V}(\mu_y)}$ (middle); solid contours for every 5 m from 10 m and dashed contours for 5 m. (right) Potential predictability contoured as in Fig. 1.

FIG. 3. As in Fig. 1, but for U300 based on the NCEP–NCAR reanalyses. (left) $\sqrt{V(\varepsilon_{yo})}$ and (middle) $\sqrt{V(\mu_y)}$; contoured every 1 m s^{-1} and dashed for 0.5 m s^{-1}. (right). Potential predictability contoured as in Fig. 1.

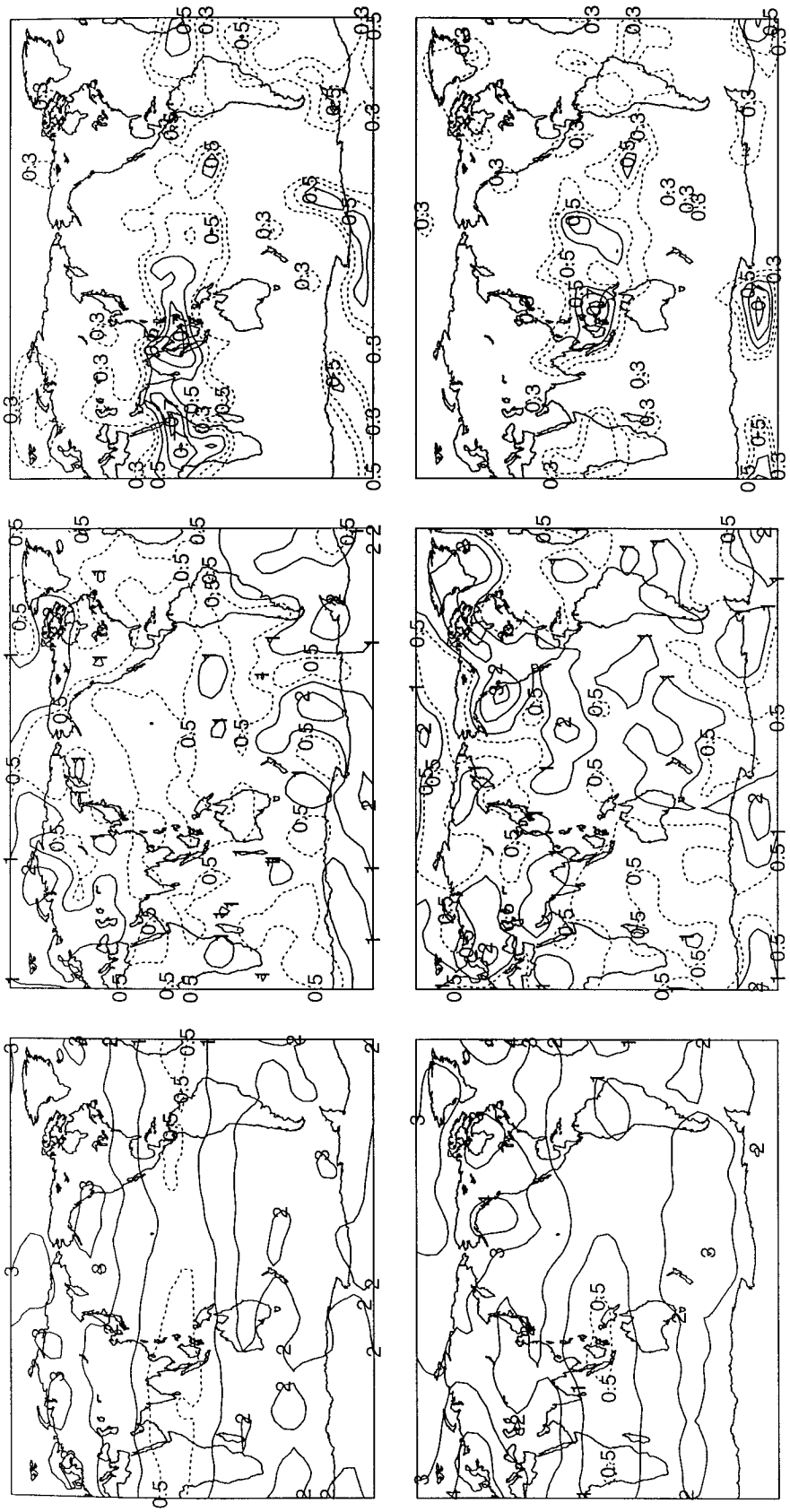

FIG. 4. As in Fig. 3, but for V300.

tended jet in DJF and double Pacific jets in JJA (Trenberth 1982).

Since the forced component of variability is much more pronounced in U300 than in V300, the potential predictability is generally higher in U300 than that in V300. Although somewhat less marked than in Z500, the potential predictability of U300 and V300 exhibits a considerable tropical–extratropical contrast with higher predictability in the Tropics. As for Z500, the meridional contrast is attributed, in part, to a stronger signal of the weather noise component in midlatitudes. In the Tropics, the pattern of the potential predictability of U300 is particularly reminiscent of ENSO signal, with a broad maximum across the equatorial Pacific. Since the forced seasonal anomalies associated with ENSO are particularly evident in the Walker circulation, the potential predictability in the Tropics is higher for U300 than for V300 in spite of the stronger weather noise component in the former. The remote influence of ENSO through the anomalous Walker cells contributes to the high predictability in the tropical Atlantic and Indian Oceans. Teleconnection of the ENSO signal results in the strong forced variability in U300 over the extratropical Pacific of the winter hemisphere, which leads to the modestly high predictability in U300 there.

4. Conclusions

A reliable method for estimating the intermonthly correlation using monthly data is proposed. This leads to a new estimation of the weather noise variability based only on monthly data. By applying the proposed method, it is apparent that monthly time series can be used successfully to partition seasonal-mean variability into the weather noise and forced and internal source components without any information derived from daily data (cf. Zwiers 1987; Zwiers 1996).

Compared with techniques based on daily time series, the method described here exhibits not only higher computational and data-handling efficiencies but also broader applicability. It was previously not possible to estimate the interannual variance due to the weather noise component either of surface temperature over a multidecadal or centennial period, where daily data are not available for much of the period, or of wind components (e.g., U300, V300), whose frequency distribution based on daily sampling is far from normally distributed. Many studies address the potential predictability of regional surface air temperatures, for example, over North America (Madden and Shea 1978; Shea and Madden 1990), Australia (Nicholls 1983), and New Zealand (Madden and Kidson 1997), but to date none have addressed global predictability because long-term global daily temperature fields are not available.

Recognizing that the weather noise component is, by nature, unpredictable on seasonal and interannual timescales, we attempted to assess the potential predictability as the ratio of the forced and internal source components to the weather noise component. Based on the multidecadal records, we found the potential predictability of surface temperature to be high over the tropical oceans and subtropical and midlatitude oceans in the winter hemisphere. Otherwise, the predictability is low, particularly over wintertime continents. Much stronger latitudinal dependencies appear in the potential predictability of the mid- and upper-tropospheric circulation. It is high only in the Tropics, where the weather noise components are weak and where seasonal anomalies tend to be coupled strongly with the underlying SST. The overall characteristics of the potential predictability of the variables studied, such as the geographical and seasonal dependencies, seem physically reasonable and consistent with current understanding.

Yet, the statistical model (2) used in our assessment is by no means perfect. For instance, the variability due to the weather noise component in our estimation may include the atmospheric response to SST fluctuations from one month to another within a season. The response should possess a certain level of potential predictability, although it is still unknown what fraction of the observed month-to-month variability in the atmosphere is accounted for by that response (Madden 1983; Shukla 1983). The imposition of a linear trend (perhaps to describe radiative forcing changes) may be somewhat limiting. It is proposed to extend the model in future to include nonlinear trend terms.

Acknowledgments. This study was initiated during a visit of one of the authors (XZ) to the Institute of Statistical Mathematics (ISM) in Tokyo under the support of a Visiting Fellowship offered by the Japanese Ministry of Education, Science, Sports and Culture. XZ thanks Prof. T. Ozaki of ISM for his hospitality. The study has been continued under the support of the Foundation for Research Science and Technology of New Zealand under Contract CO1628. The surface temperature data we used were obtained from the Climate Research Unit, University of East Anglia and the reanalysis data from the NCAR Data Support Section. We wish to thank Dr. F. Zwiers and the two anonymous reviewers for their valuable comments.

APPENDIX A

Proofs of Formulas in Table 1

Consider the statistical model of monthly means given in (1). Here, we assume that their intermonthly fluctuations within each 3-month season arise solely from the weather noise component, that is,

$$\begin{cases} x_{y1} - x_{y2} = \varepsilon_{y1} - \varepsilon_{y2}, \\ x_{y2} - x_{y3} = \varepsilon_{y2} - \varepsilon_{y3}, \end{cases} \qquad y = 1, \ldots, Y. \quad \text{(A1)}$$

Under the assumptions (3), (4), and (5), the variance matrix of monthly means of the weather noise component $\{\varepsilon_{y1}, \varepsilon_{y2}, \varepsilon_{y3}\}$ may be expressed as

$$\mathbf{V}_{\varepsilon} = E\begin{pmatrix}\varepsilon_{y1}\\ \varepsilon_{y2}\\ \varepsilon_{y3}\end{pmatrix}(\varepsilon_{y1} \quad \varepsilon_{y2} \quad \varepsilon_{y3}) = \sigma^2\begin{pmatrix}1 & \rho_1 & 0\\ \rho_1 & 1 & \rho_1\\ 0 & \rho_1 & 1\end{pmatrix},$$

where E denotes the expectation value based on the all Y years, σ^2 the interannual variance of ε_{ym}, and $\rho_1 = C(\varepsilon_{y1}, \varepsilon_{y2}) = C(\varepsilon_{y2}, \varepsilon_{y3})$ the correlation coefficient of ε_{ym} between two adjacent months. Likewise, the variance matrix of the intermonthly fluctuations of $\{\varepsilon_{y1} - \varepsilon_{y2}, \varepsilon_{y2} - \varepsilon_{y3}\}$ may be written as

$$\mathbf{V}_{d\varepsilon} = E\begin{pmatrix}\varepsilon_{y1} - \varepsilon_{y2}\\ \varepsilon_{y2} - \varepsilon_{y3}\end{pmatrix}(\varepsilon_{y1} - \varepsilon_{y2} \quad \varepsilon_{y2} - \varepsilon_{y3})$$

$$= \sigma^2\begin{pmatrix}2 - 2\rho_1 & 2\rho_1 - 1\\ 2\rho_1 - 1 & 2 - 2\rho_1\end{pmatrix}.$$

Therefore the -2 ln (logarithmic) likelihood for (A1) becomes (Jones 1993)

$$L(\rho_1, \{x_{ym}\}) = Y\{2[\ln(2\pi\hat{\sigma}) + 1] + \ln[\det(\mathbf{V}_{d\varepsilon})]\},$$

where the estimated variance is given by

$$\hat{\sigma}^2 = \frac{1}{2Y}\sum_{y=1}^{Y}(x_{y1} - x_{y2} \quad x_{y2} - x_{y3})\mathbf{V}_{d\varepsilon}^{-1}\begin{pmatrix}x_{y1} - x_{y2}\\ x_{y2} - x_{y3}\end{pmatrix}. \quad \text{(A2)}$$

Since the determinant and inverse of $\mathbf{V}_{d\varepsilon}$ are given by

$$\det(\mathbf{V}_{d\varepsilon}) = 3 - 4\rho_1 \quad \text{and}$$

$$\mathbf{V}_{d\varepsilon}^{-1} = \frac{1}{\det(\mathbf{V}_{d\varepsilon})}\begin{pmatrix}2 - 2\rho_1 & 1 - 2\rho_1\\ 1 - 2\rho_1 & 2 - 2\rho_1\end{pmatrix},$$

respectively, we find after some algebraic manipulations that $L(\rho_1, \{x_{ym}\})$ is minimized for $\rho_1 = 1.5 - \upsilon_1/\upsilon_2$, where specific expressions of υ_1 and υ_2 are given in Table 1. Then, the constraint $0 \le \rho_1 \le 0.1$ based on the discussion in section 2b is imposed on ρ_1, which leads to the particular expression for $C(\varepsilon_{y1}, \varepsilon_{y2})$ (i.e., ρ_1) shown in Table 1. By substituting ρ_1 in (A2) by the estimated $C(\varepsilon_{y1}, \varepsilon_{y2})$, we obtain

$$\hat{V}(\varepsilon_{ym}, \varepsilon_{ym}) = \hat{\sigma}^2 = \frac{[-2\upsilon_2\hat{C}(\varepsilon_{y1}, \varepsilon_{y2}) + 2\upsilon_1]}{[3 - 4\hat{C}(\varepsilon_{y1}, \varepsilon_{y2})]} \quad \text{and}$$

$$\hat{V}(\varepsilon_{yo}) = \frac{1}{9}\sum_{i,j=1}^{3}\hat{V}(\varepsilon_{yi}, \varepsilon_{yj}) = \frac{\hat{V}(\varepsilon_{y1})[3 + 4\hat{C}(\varepsilon_{y1}, \varepsilon_{y2})]}{9},$$

both of which are also shown in Table 1.

Zwiers (1996) showed how to estimate the intermonth correlation coefficients given an estimated 1-day lag correlation and how to incorporate them into monthly data for estimating $\hat{V}(\varepsilon_{yo})$. The key innovation here is that the intermonth correlation is estimated from monthly data but not daily data. Once the intermonth correlation is known, our estimation for $\hat{V}(\varepsilon_{yo})$ is essentially identical to that proposed by Zwiers (1996). Especially, $\hat{V}(\varepsilon_{yo})$ is approximately distributed as $\chi^2(T^*Y)V(\varepsilon_{yo})/[T^*Y]$, where

$$T^* = \frac{2(3 - 2\rho_1)^2}{9 - 12\rho_1 + 8\rho_1^2}. \quad \text{(A3)}$$

APPENDIX B

Comparison with Frequency Domain Method

If daily data are available, they can be assumed to have the regression form

$$x_{yt} = \mu_y + \varepsilon_{yt} \qquad (t = 1, \ldots, T), \quad \text{(B1)}$$

where ε_{yt} is a weather noise anomaly on day t in year y, and T (=90) is the number of days *within* a 3-month season (Zheng 1996). If the daily time series associated with the weather noise component $\{\varepsilon_{yt}, t = 1, \ldots, T\}$ is stationary, the interannual variability of the seasonal mean arising from the weather noise component can be estimated from the variance spectrum of ε_{yt} as

$$\hat{V}(\varepsilon_{yo}) = \frac{1}{Y \times T^2}\sum_{y=1}^{Y}\left|\sum_{t=1}^{T}x_{yt}e^{i2\pi t/T}\right|^2, \quad \text{(B2)}$$

where i stands for the imaginary unit (Zwiers 1987).

The following simulation was carried out in order to verify the proposed estimation method against the above frequency domain method. A synthetic dataset comprising 40 independent AR(1) time series with length 90 (days) was generated using the Splus routine ''arima.sim'' (StatSci 1993). For each AR(1) series, the first-order autoregressive coefficient α was set to be 0.4, 0.6, and 0.8 in turn. The innovation variance was held constant at 1 throughout. In total, 100 such independent synthetic datasets were generated. Both analysis meth-

TABLE B1. Simulation results using 40 yr of synthetic data (Y = 40). The ''traditional'' method refers to Zwiers (1987) as shown in (B2) of appendix B. ''Proposed'' is the method described in this paper. The other two methods are variations of the proposed method as described in appendix C. Column 2 indicates the degree of daily autocorrelation in the time series. Columns 3 and 4 indicate how well the weather noise variability is estimated. The perfect values for them are one (i.e., no bias) and 0.158 [i.e., $\hat{V}(\varepsilon_{yo})$ is distributed as $\chi^2(80)V(\varepsilon_{yo})/80$], respectively.

Estimation method for $V(\varepsilon_o)$	α for daily AR(1) series	$\frac{E[\hat{V}(\varepsilon_{yo})]}{V(\varepsilon_{yo})}$	$\frac{\sqrt{V[\hat{V}(\varepsilon_{yo})]}}{V(\varepsilon_{yo})}$
Traditional	0.4	0.97	0.16
Proposed		1.01	0.18
Unconstrained		0.92	0.49
$C(\varepsilon_{y1}, \varepsilon_{y2}) = 0$		0.93	0.15
Traditional	0.6	0.99	0.17
Proposed		0.99	0.19
Unconstrained		0.93	0.51
$C(\varepsilon_{y1}, \varepsilon_{y2}) = 0$		0.91	0.15
Traditional	0.8	0.92	0.14
Proposed		0.92	0.16
Unconstrained		1.00	0.40
$C(\varepsilon_{y1}, \varepsilon_{y2}) = 0$		0.83	0.12

ods were applied to each synthetic dataset to estimate $V(\varepsilon_{yo})$. The theoretical variance of ε_{yo} is

$$V(\varepsilon_{yo}) = \frac{\sigma^2}{T(1-\alpha^2)}\left[1 + 2\sum_{t=1}^{T}(1 - t/T)\alpha^t\right]. \quad \text{(B3)}$$

The mean and standard deviation of the 100 members of $\hat{V}(\varepsilon_{yo})$ (denoted as $E[\hat{V}(\varepsilon_{yo})]$ and $\sqrt{V[\hat{V}(\varepsilon_{yo})]}$, respectively) normalized by $\sqrt{V(\varepsilon_{yo})}$ are listed in Table B1. For each of the values of α, no significant differences are found in either of those two statistics between its estimations based on the (traditional) frequency domain method and the method proposed in this study. The two estimation methods both yield $E[\hat{V}(\varepsilon_{yo})]/V(\varepsilon_{yo})$ close to unity and $\sqrt{V[\hat{V}(\varepsilon_{yo})]}/V(\varepsilon_{yo})$ close to 0.158 (the theoretical value when $\hat{V}(\varepsilon_{yo})$ is distributed as $\chi^2(80)V(\varepsilon_{yo})/80$), indicating that the bias and error introduced in either of the two methods both tend to be small.

APPENDIX C

Constraints on $C(\varepsilon_{y1}, \varepsilon_{y2})$

The proposed method is again applied to each synthetic dataset in the same manner as in appendix B for estimating $V(\varepsilon_{yo})$ but with the following two modifications applied to $\hat{C}(\varepsilon_{y1}, \varepsilon_{y2})$: (a) no constraint: that is, $\hat{C}(\varepsilon_{y1}, \varepsilon_{y2}) = 1.5 - v_1/v_2$, and (b) constrained as zero: that is, $\hat{C}(\varepsilon_{y1}, \varepsilon_{y2}) = 0$. All results are included in Table B1.

The modification (a) is designed to check the importance of the constraint that limits $\hat{C}(\varepsilon_{y1}, \varepsilon_{y2})$ below 0.1. Table B1 shows that without this constraint the ratio $\sqrt{V[\hat{V}(\varepsilon_{yo})]}/V(\varepsilon_{yo})$ is between 0.4 and 0.5, which is much larger than that based on other methods (around 0.15). Hence, constraining $\hat{C}(\varepsilon_{y1}, \varepsilon_{y2})$ between 0 and 0.1 is an important step toward reducing estimation errors.

The modification (b) is designed to examine the relevance of assuming the weather noise component to be completely independent from one month to another, which could simplify the estimation substantially (Zwiers 1996). Although this constraint acts to reduce estimation errors slightly regardless of the values of the AR(1) coefficient (Table B1), it gives rise to a considerable negative bias, especially for the time series with the relatively large coefficient (i.e., $\alpha = 0.8$). With these reasonable results, we conclude that appropriate estimation of the intermonthly correlation of the weather noise component is important in estimating its interannual variability, especially for such a daily time series with relatively high persistency as that of SST or even atmospheric variables in the Tropics.

APPENDIX D

An Example for Meteorological Data

We have analyzed DJF Z500 using both the traditional and proposed methods. The results are shown in Fig.

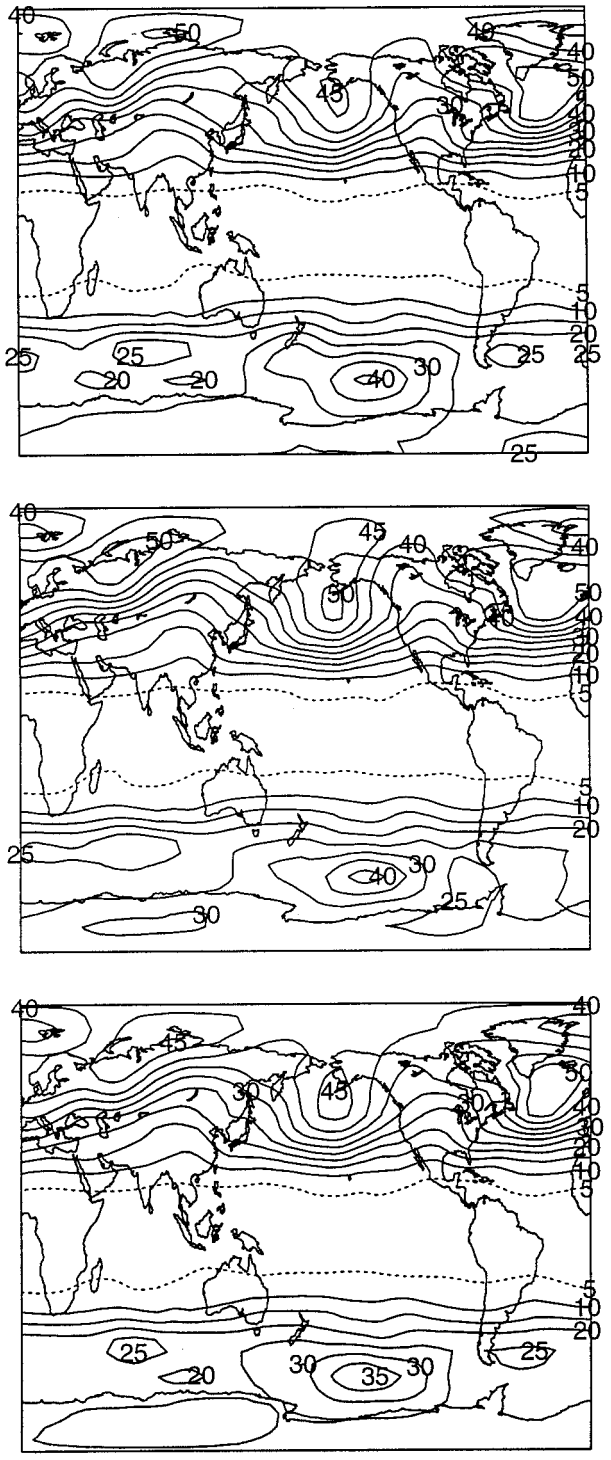

FIG. D1. Here $\sqrt{\hat{V}(\varepsilon_{yo})}$ for Z500. The top, middle, and bottom panels are derived from the traditional method, the proposed method, and the proposed method with the constraint $C(\varepsilon_{y1}, \varepsilon_{y3}) = 0$, respectively. Solid contours for every 5 m from 10 m and dashed contours for 5 m.

D1. Overall, $\sqrt{\hat{V}(\varepsilon_{yo})}$ derived from the daily data (top panel) coincides well with $\sqrt{\hat{V}(\varepsilon_{yo})}$ derived from the monthly means (middle panel). However, the former is less than the latter over the ocean areas, especially over the North Pacific, although the general pattern is very similar.

For the North Pacific, $\sqrt{\hat{V}(\varepsilon_{yo})}$ derived from the monthly means with the constraint $C(\varepsilon_{y1}, \varepsilon_{y2}) = 0$ (bottom) is about the same as that derived from the traditional approach, but less than that derived from the proposed approach. Since the daily autocorrelation coefficients over North Pacific are more than 0.8, with the reasoning given in appendix C, $\sqrt{\hat{V}(\varepsilon_{yo})}$ derived with the independence constraint is negatively biased, so that $\sqrt{\hat{V}(\varepsilon_{yo})}$ derived from the traditional approach must be underestimated over the North Pacific, especially in the Aleutian region. Therefore, the difference between the middle and top panels in Fig. D1 over the North Pacific does not necessarily indicate that the estimates derived from the proposed approach are wrong. The underlying reasons for the magnitude difference are subject to further investigation.

REFERENCES

Alexander, M. A., and C. Deser, 1995: A mechanism for the recurrence of wintertime midlatitude SST anomalies. *J. Climate,* **8,** 122–137.

Basher, R. E., and C. S. Thompson, 1996: Relationship of air temperature in New Zealand to regional anomalies in sea-surface temperature and atmospheric circulation. *Int. J. Climatol.,* **16,** 405–425.

Bjerknes, J., 1969: Atmospheric teleconnection from the equatorial Pacific. *Mon. Wea. Rev.,* **97,** 163–172.

Blackmon, M. L., 1976: A climatological spectral study of the 500-mb geopotential height of the Northern Hemisphere. *J. Atmos. Sci.,* **33,** 1607–1623.

——, Y.-H. Lee, and J. M. Wallace, 1984: Horizontal structure of 500-mb height fluctuations with long, intermediate, and short time scales. *J. Atmos. Sci.,* **41,** 961–979.

Cane, M. A., 1986: El Niño. *Ann. Rev. Earth Planet. Sci.,* **14,** 43–70.

Cayan, D. R., 1980: Large-scale relationships between sea surface temperature and surface air temperature. *Mon. Wea. Rev.,* **108,** 1293–1301.

Epstein, E. S., 1991: Determining the optimum number of harmonics to represent normals based on multiyear data. *J. Climate,* **4,** 1047–1051.

Hoerling, M. P., and M. Ting, 1994: Organization of extratropical transients during El Niño. *J. Climate,* **7,** 745–766.

Holton, J. R., 1992: *An Introduction to Dynamic Meteorology.* 3d ed. International Geophysics Series, Vol. 48, Academic Press, 511 pp.

Honda, M., K. Yamazaki, H. Nakamura, and K. Takeuchi, 1999: Dynamic and thermodynamic characteristics of atmospheric response to anomalous sea-ice extent in the Sea of Okhotsk. *J. Climate,* **12,** 3347–3358.

Horel, J. D., and J. M. Wallace, 1981: Planetary-scale atmospheric phenomena associated with the Southern Oscillation. *Mon. Wea. Rev.,* **109,** 813–829.

Hurrel, J. W., 1995: Transient eddy forcing of the rotational flow during northern winter. *J. Atmos. Sci.,* **52,** 2286–2301.

Iwasaka, N., J. Hanawa, and Y. Yoba, 1987: Analysis of SST anomalies in the North Pacific and their relation to 500 mb height anomalies over the Northern Hemisphere during 1969–1979. *J. Meteor. Soc. Japan,* **65,** 103–114.

Jones, P. D., 1996: Hemispheric and global temperatures, 1851–1996. Part 1. *Climate Monit.,* **25,** 20–30.

Jones, R. H., 1975: Estimating the variance of time averages. *J. Appl. Meteor.,* **14,** 159–163.

——, 1993: *Longitudinal Data with Serial Correlation: A State-Space Approach.* Chapman and Hall, 225 pp.

Kalnay, E., and Coauthors, 1996: The NCEP/NCAR 40-year reanalysis project. *Bull. Amer. Meteor. Soc.,* **77,** 437–471.

Kidson, J. W., 1999: Principal modes of Southern Hemisphere low-frequency variability obtained from NCEP–NCAR reanalyses. *J. Climate,* **12,** 2808–2830.

Kleeman, R., and A. M. Moore, 1997: A theory for the limitation of ENSO predictability due to stochastic atmospheric transients. *J. Atmos. Sci.,* **54,** 753–767.

Kushnir, Y., and J. M. Wallace, 1989: Low-frequency variability in the Northern Hemisphere winter: Geographical distribution, structure and time-scale dependence. *J. Atmos. Sci.,* **46,** 3122–3142.

Lau, N.-C., 1988: Variability of the observed midlatitude stormtracks in relation to low-frequency changes in the circulation pattern. *J. Atmos. Sci.,* **45,** 2718–2743.

——, and M. J. Nath, 1991: Variability of the baroclinic and barotropic transient eddy forcing associated with monthly changes in the midlatitude storm tracks. *J. Atmos. Sci.,* **48,** 2589–2613.

——, and ——, 1994: A modeling study of the relative roles of the tropical and extratropical SST anomalies in the variability of the global atmosphere–ocean system. *J. Climate,* **7,** 1184–1207.

Leith, C. E., 1973: The standard error of time-average estimates of climatic means. *J. Appl. Meteor.,* **12,** 1066–1069.

Lorenz, E. N., 1970: Climate change as a mathematical problem. *J. Appl. Meteor.,* **9,** 325–329.

Madden, R. A., 1976: Estimates of the natural variability of time averaged sea level pressure. *Mon. Wea. Rev.,* **104,** 942–952.

——, 1981: A quantitative approach to long-range prediction. *J. Geophys. Res.,* **86,** 9817–9825.

——, 1983: Reply. *Mon. Wea. Rev.,* **111,** 586–589.

——, and P. R. Julian, 1971: Detection of a 40–50 day oscillation in the zonal wind in the tropical Pacific. *J. Atmos. Sci.,* **28,** 702–708.

——, and ——, 1972: Detection of global-scale circulation cells in the tropics with a 40–50 day period. *J. Atmos. Sci.,* **29,** 1109–1123.

——, and D. J. Shea, 1978: Estimates of the natural variability of time-averaged temperatures over the United States. *Mon. Wea. Rev.,* **106,** 1695–1703.

——, and J. W. Kidson, 1997: The potential long-range predictability of temperature over New Zealand. *Int. J. Climatol.,* **17,** 483–495.

Manabe, S., R. J. Stouffer, M. J. Spelman, and K. Bryan, 1991: Transient responses of a coupled ocean–atmosphere model to gradual changes of atmospheric CO_2. Part I: Annual mean response. *J. Climate,* **4,** 785–818.

——, M. J. Spelman, and R. J. Stouffer, 1992: Transient responses of a coupled ocean–atmosphere model to gradual changes of atmospheric CO_2. Part II: Seasonal response. *J. Climate,* **5,** 105–126.

Nakamura, H., and T. Yamagata, 1999: Recent decadal SST variability in the Northwestern Pacific and associated atmospheric anomalies. *Beyond El Niño: Decadal and Interdecadal Climate Variability,* A. Navarra, Ed., Springer, 49–72.

Nicholls, N., 1983: The potential for long-range prediction of seasonal mean temperature in Australia. *Aust. Meteor. Mag.,* **31,** 203–207.

Rao, C. R., 1973: *Linear Statistical Inference and Its Applications.* John Wiley and Sons, 625 pp.

Rasmusson, E. M., and T. H. Carpenter, 1982: Variations in tropical sea surface temperature and surface wind fields associated with the Southern Oscillation/El Niño. *Mon. Wea. Rev.,* **110,** 354–384.

Renwick, J. A., 1998: ENSO-related variability in the frequency of South Pacific blocking. *Mon. Wea. Rev.,* **126,** 3117–3123.
Rowntree, P. R., 1972: The influence of the tropical east Pacific Ocean temperature on the atmosphere. *Quart. J. Roy. Meteor. Soc.,* **98,** 290–321.
Shea, D. J., and R. A. Madden, 1990: Potential for long-range prediction of monthly mean surface temperatures over North America. *J. Climate,* **3,** 1444–1451.
Shukla, J., 1983: Comments on ''Natural variability and predictability.'' *Mon. Wea. Rev.,* **111,** 581–585.
——, 1998: Predictability in the midst of chaos: A scientific basis for climate forecasting. *Science,* **282,** 728–731.
Sinclair, M. R., 1996: A climatology of anticyclones and blocking for the Southern Hemisphere. *Mon. Wea. Rev.,* **124,** 245–263.
StatSci., 1993: *S-PLUS* Guide to Statistical and Mathematical Analysis Version 3.2. Statistical Sciences, 630 pp.
Trenberth, K. E., 1981: Observed Southern Hemisphere eddy statistics at 500 mb: Frequency and spatial dependence. *J. Atmos. Sci.,* **38,** 2585–2605.
——, 1982: Seasonality in Southern Hemisphere eddy statistics at 500 mb. *J. Atmos. Sci.,* **39,** 2507–2520.
——, 1984: Some effects of finite sample size and persistence on meteorological statistics. Part II: Potential predictability. *Mon. Wea. Rev.,* **112,** 2369–2379.
van Loon, H., and J. C. Rodgers, 1978: The seesaw in winter temperatures between Greenland and Northern Europe. Part I: General description. *Mon. Wea. Rev.,* **106,** 296–310.
Wallace, J. M., and D. S. Gutzler, 1981: Teleconnections in the geopotential height field during the Northern Hemisphere winter. *Mon. Wea. Rev.,* **109,** 784–812.
White, W. B., and R. G. Peterson, 1996: An Antarctic circumpolar wave in surface pressure, wind, temperature and sea-ice extent. *Nature,* **380,** 699–702.
Zheng, X., 1996: Unbiased estimation of autocorrelations of daily meteorological variables. *J. Climate,* **9,** 2197–2203.
——, and C. S. Frederiksen, 1999: Validating interannual variability in an ensemble of AGCM simulations. *J. Climate,* **12,** 2386–2396.
Zwiers, F. W., 1987: A potential predictability study conducted with an atmospheric general circulation model. *Mon. Wea. Rev.,* **115,** 2957–2974.
——, 1996: Interannual variability and predictability in an ensemble of AMIP climate simulations conducted with the CCC GCM2. *Climate Dyn.,* **12,** 825–847.
——, and H. von Storch, 1995: Taking serial correlation into account in tests of mean. *J. Climate,* **8,** 336–351.